Article of investigation

SEPIC converter: modeling and control considering internal energy losses

El convertidor Sepic: modelado y control usando elementos 2 no ideales

Luis D. Patarroyo-Gutiérrez[1] Mario E. González-Niño[1] Jorge A. Plazas[1]

[1]Universidad Pedagógica y Tecnológica de Colombia, Tunja – Colombia.

Abstract

This paper describes a procedure for designing a 2-kilowatt SEPIC converter controller without ideal devices, to be used in industrial applications. A small-signal model can be constructed from a commuted converter in different operation modes. Subsequently, a transfer function is determined to design the analog controller, ensuring a settling time of 25 ms. The results around the operation point are shown using MATLAB®/SIMULINK®, and perturbations are applied to the converter output and the DC input voltage to evaluate performance in the time domain. The designed controller effectively meets the design specifications for disturbances near the operating point.

Resumen

En este artículo se describe el procedimiento que permite diseñar un controlador para un convertidor Sepic de 2 kilovatios con elementos no ideales que puede ser usado en aplicaciones industriales. Se obtiene el modelo conmutado del convertidor a partir de los modos de operación, con este se construye el modelo en pequeña señal que permite obtener la función de transferencia necesaria para el diseño del controlador análogo, garantizado un tiempo de establecimiento de 25 ms. Se muestran los resultados de simulación usando MATLAB®/SIMULINK® alrededor del punto de operación realizando perturbaciones a la salida del convertidor y variaciones en el voltaje DC de entrada, evaluando el desempeño del sistema en el dominio temporal. Con el controlador diseñado se satisface la especificación de diseño para las resistencias internas de los inductores hasta 0.3 Ohmnios.

OPEN ACCESS

Why was it carried out?
This study was carried out in order to understand the mathematical modeling of power electronic converters and its application to the design of linear controllers.

What were the most relevant results?
The simulation results demonstrated that the temporal response of the proposed mathematical model is close to the response of the circuit with discrete elements simulated in MATLAB. Consequently, the variance in the voltage of the controller stress signals in the exposed cases is less than 3 mV.

What do these results provide?
The results of this research demonstrate that the mathematical procedure used is capable of obtaining the small signal model, including energy losses, in a structured way, providing results close to the temporal response of the power electronic converter circuit.

Graphical Abstract
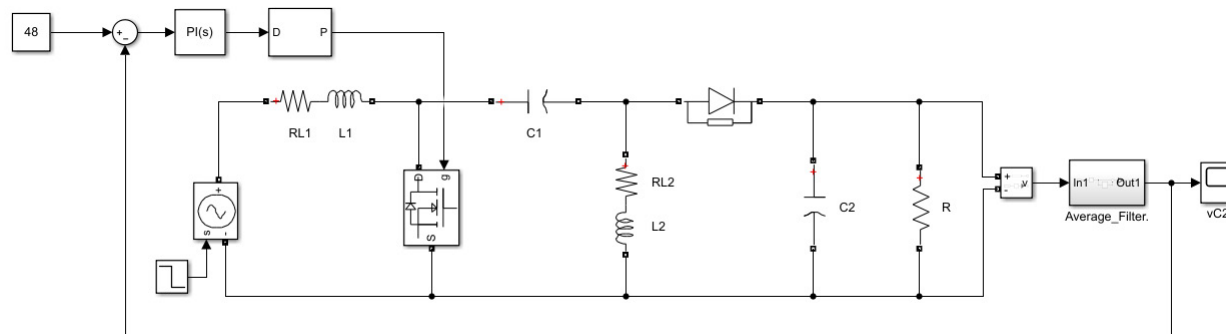
Introduction

Direct current (DC-DC) converters are used in applications that require voltage step-up or step-down, contingent upon the topology of each converter. The SEPIC converter, for instance, facilitates both voltage boosting and bucking, rendering it suitable for renewable energy applications, where it maintains regulation over output DC voltage levels [1]. One such converter application is the implementation of Maximum Power Point Tracking (MPPT) in photovoltaic or wind generation systems, accomplished through control strategies [2]. Understanding the mathematical models that represent converter dynamics is crucial for designing controllers capable of meeting the specific requirements of the intended applications. A converter may be represented by transfer functions, as in [3,4], where the ratios between duty cycle and output voltage, as well as between the input voltage to output voltage are presented. These transfer functions enable the identification of the converter's response to disturbances in each of its parameters or characteristics. Another representation is the switched model, which comprehensively describes the behavior of a converter and is derived from the operating modes [5,6,7,8,9,10,11,12,13,14]. This model is useful for obtaining the converter's small-signal model [4,6,11,13,15,16], which is essential for designing linear controllers [17]. In the reviewed literature, most authors obtain models using ideal elements, while in [5,18–20] the authors propose transfer functions and switched models with non-ideal elements, providing models that are more approximate to the implemented circuit. However, they do not provide control actions for the converter.

In converter control, output voltage regulation is commonly implemented [3,7,11–13,15,16,21,22], to ensure that the converter maintains an approximately constant output voltage despite fluctuations in the input voltage supplying the converter or variations in connected load.

As a contribution to the literature review, this article introduces the small-signal mathematical model of the SEPIC converter, incorporating the internal resistances of the inductors. Using this non-ideal model, an analog PI controller is proposed to regulate the output DC voltage.

The rest of the paper is structured as follows. In Section 2, the converter operation modes are presented. Following this, Section 3 demonstrates the converter switched model. Section 4 details the small-signal model. The controller designed for the converter is discussed in Section 5. The simulation results of the controlled converter model, accounting for variations in both input voltages and loads are given in Section 6. Finally, conclusions drawn from the analysis of results and compliance with the specifications defined for the performance of the SEPIC converter are presented.

Operation modes

The SEPIC converter can raise or lower the output voltage levels. This feature enables the regulation of changes in DC levels in photovoltaic farms [1]. Figure 1 shows the SEPIC converter, which consists of four elements that store energy: two inductors with internal resistances, two capacitors, a MOSFET, a Diode and a resistor.
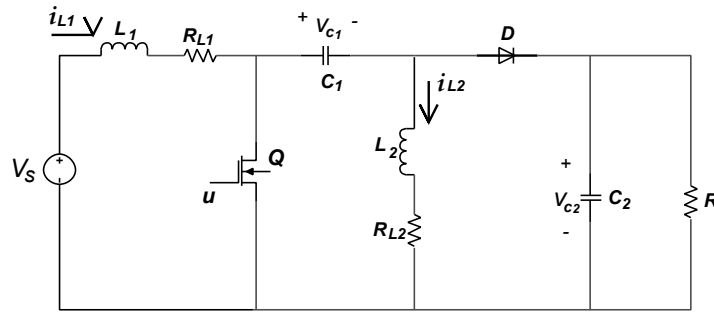
Figure 1. SEPIC converter.

This converter has two configurations based on the switching states of the MOSFET. When the MOSFET is in the activation state, configuration I is presented, whereas, upon deactivation, configuration II is established, as depicted in Figure 2.

In configuration I, the MOSFET is switched on and current flows through it, the source V_s, the inductor L_1, and the resistor R_{L1}, As a result, the source charges the inductor L_1. An effect of this activation is that the circuit diode turns off; consequently, condenser C_2 supplies energy to the output resistance. When the control signal deactivates the MOSFET, configuration II appears as observed in Figure 2b. The diode is activated because the voltage at the anode terminal is higher resulting from the addition of the voltages of the source and the charged inductor. By applying Kirchhoff's voltage and current laws in the configurations, the switched model is constructed, as presented in the following section.
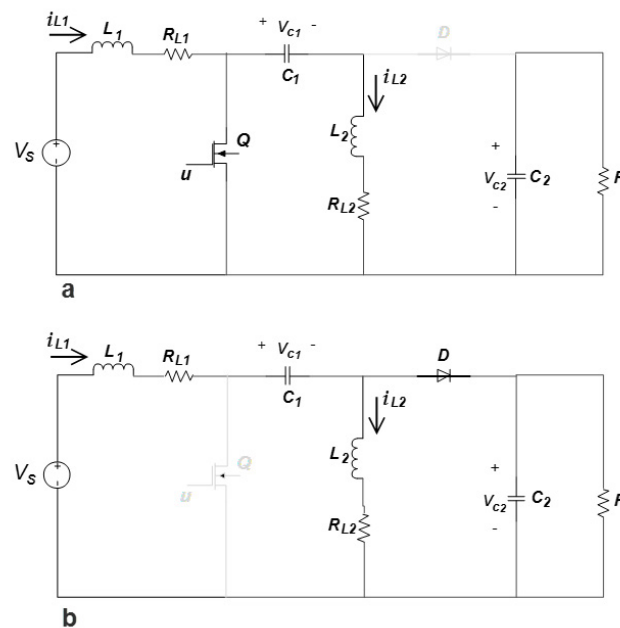

Figure 2. (a) converter with active control signal. (b) converter with non-active control signal.

Switched model

The switched model of the SEPIC converter is constructed using the state variables, which include the currents i_{L1}, i_{L2} in the inductors L_1 and L_2, respectively, along with the voltages v_{C1} and v_{C2} accross the condensers C_1 and C_2, respectively.

In Configuration I, the voltages and currents required to obtain the state equations are determined from Eq. (1). For configuration II, the state equations are presented in Eq. (2)

$$\frac{di_{L_1}}{dt} = \frac{1}{L_1} \cdot V_s - \frac{R_{L1}}{L_1} \cdot i_{L_1}$$

$$\frac{dv_{C_1}}{dt} = \frac{1}{C_1} \cdot i_{L_2}$$

$$\frac{di_{L_2}}{dt} = -\frac{R_{L2}}{L_2} \cdot i_{L_2} - \frac{1}{L_2} \cdot v_{C1}$$ (1)

$$\frac{dv_{C_2}}{dt} = -\frac{1}{R \cdot C_2} \cdot v_{C2}$$

$$\frac{di_{L_1}}{dt} = \frac{1}{L_1} \cdot V_s - \frac{R_{L1}}{L_1} \cdot i_{L_1} - \frac{1}{L_1} \cdot (v_{C1} + v_{C2})$$

$$\frac{dv_{C_1}}{dt} = \frac{1}{C_1} \cdot i_{L_1}$$

$$\frac{di_{L_2}}{dt} = -\frac{R_{L2}}{L_2} \cdot i_{L_2} + \frac{1}{L_2} \cdot v_{C2}$$ (2)

$$\frac{dv_{C_2}}{dt} = \frac{1}{C_2} (i_{L_1} - i_{L_2}) - \frac{1}{R \cdot C_2} \cdot v_{C2}$$

The switched model in state space for the SEPIC converter is constructed by grouping Eq. (1) and Eq. (2). The result is presented in Eq. (3). The control signal $d(t)$ is 1 when the MOSFET must be activated and 0 otherwise.

$$L_1 \cdot \frac{di_{L_1}}{dt} = V_s - R_{L1} \cdot i_{L_1} - (v_{C1} + v_{C2}) \cdot (1 - d)$$

$$C_1 \cdot \frac{dv_{C_1}}{dt} = i_{L_2} \cdot d + i_{L_1} \cdot (1 - d)$$

(3)

$$L_2 \cdot \frac{di_{L_2}}{dt} = -R_{L2} \cdot i_{L_2} - v_{C1} \cdot d + v_{C2} \cdot (1 - d)$$

$$C_2 \cdot \frac{dv_{C_2}}{dt} = (i_{L_1} - i_{L_2}) \cdot (1 - d) - \frac{1}{R} \cdot v_{C2}$$

To derive the average model, the moving average of Eq. (3) must be calculated, replacing the switching signal d with its average, defined as α. The average model of the SEPIC converter in state space is presented in Eq. (4).

$$L_1 \cdot \frac{di_{L_1}}{dt} = V_s - R_{L1} \cdot i_{L_1} - (v_{C1} + v_{C2}) \cdot (1 - \alpha)$$

$$C_1 \cdot \frac{dv_{C_1}}{dt} = i_{L_2} \cdot \alpha + i_{L_1} \cdot (1 - \alpha)$$

(4)

$$L_2 \cdot \frac{di_{L_2}}{dt} = -R_{L2} \cdot i_{L_2} - v_{C1} \cdot \alpha + v_{C2} \cdot (1 - \alpha)$$

$$C_2 \cdot \frac{dv_{C_2}}{dt} = (i_{L_1} - i_{L_2}) \cdot (1 - \alpha) - \frac{1}{R} \cdot v_{C2}$$

Small-signal model

The small-signal model is defined based on the average model, the converter equilibrium points, and the variations around the operating point in each of the state variables. The following are the steps and equations that enable the calculation of each of these aspects, culminating in the presentation of the small-signal model.

The equilibrium points are calculated by setting Eq. (4) to zero, and solving for each value of i_{L1}, i_{L2}, v_{C1} and v_{C2}. The subscript e is added to indicate each value of current and voltage at the equilibrium point. These are presented in Eq. (5), enabling the determination of the steady-state response to each state variable of the SEPIC converter.

$$i_{L1e} = \frac{V_s \alpha_e^2}{(R + R_{L2})(1 - \alpha_e)^2 - R_{L1}\alpha_e^2}$$

$$i_{L2e} = \frac{V_s \alpha_e(1 - \alpha_e)}{(R + R_{L2})(1 - \alpha_e)^2 - R_{L1}\alpha_e^2}$$

(5)

$$v_{C1e} = \frac{V_s(R + R_{L2})(1 - \alpha_e)^2}{(R + R_{L2})(1 - \alpha_e)^2 - R_{L1}\alpha_e^2}$$

$$v_{C2e} = \frac{V_s \alpha_e(1 - \alpha_e)R}{(R + R_{L2})(1 - \alpha_e)^2 - R_{L1}\alpha_e^2}$$

The tilde $^{\sim}$ indicates the variations around the operation point. Eq. (6) defines the variations around the operational point for each state variable and the switching signal.

$$v_{C1} = v_{C1e} + \tilde{v}_{C1}$$

$$v_{C2} = v_{C2e} + \tilde{v}_{C2}$$

$$i_{L1} = i_{L1e} + \tilde{i}_{L1}$$

(6)

$$i_{L2} = i_{L2e} + \tilde{i}_{L2}$$

$$\alpha = \alpha_e + \tilde{\alpha}$$

The small-signal model is acquired by substituting Eq. (6) into Eq. (4), omitting terms of order higher than one (17). This model is described in Eq. (7).

$$L_1 \frac{d\widetilde{i_{L_1}}}{dt} = -R_{L1} \cdot \tilde{i}_{L1} + (v_{C1e} + v_{C2e}) \cdot \tilde{\alpha} - (1 - \alpha_e)(\tilde{v}_{C1} + \tilde{v}_{C2}) + V_s$$

$$C_1 \frac{d\widetilde{v_{C_1}}}{dt} = (i_{L2e} - i_{L1e}) \cdot \tilde{\alpha} + (1 - \alpha_e) \cdot \tilde{i}_{L1} + \alpha_e \cdot \tilde{i}_{L2}$$

(7)

$$L_2 \frac{d\widetilde{i_{L_2}}}{dt} = -R_{L2} \cdot \tilde{i}_{L2} - \alpha_e \cdot \tilde{v}_{C1} + (1 - \alpha_e) \cdot \tilde{v}_{C2} - (v_{C1e} + v_{C2e}) \cdot \tilde{\alpha}$$

$$C_2 \frac{d\widetilde{v_{C_2}}}{dt} = (1 - \alpha_e) \cdot \tilde{i}_{L1} - (1 - \alpha_e) \cdot \tilde{i}_{L2} - \frac{1}{R} \cdot \tilde{v}_{C2} - (i_{L1e} - i_{L2e}) \cdot \tilde{\alpha}$$

Controller design

The converter's design parameters are proposed for a 2-kW load power. The values for inductors and condensers are obtained from Eq. (8). These values are determined to prevent exceeding a current ripple higher than 40% in the inductors, and 1% and 2% in condenser voltages C_1 and C_2, respectively.

$$\Delta I_L = I_{out} \cdot \frac{v_{out}}{v_{in(min)}} \cdot I_{ripple}\%$$

$$L_1 = L_2 = \frac{v_{in(min)}}{\Delta I_L \cdot f_s} \cdot D_{max}$$ (8)

$$C_1 = \frac{I_{out} \cdot D_{max}}{\Delta v_{c1} \cdot f_s}$$

$$C_2 = \frac{I_{out} \cdot D_{max}}{V_{ripple} \cdot 0.5 \cdot f_s}$$

The established parameters for the converter are summarized in Table 1. These parameters are used in the converter's small-signal model described in Eq. (7). With this model, the transfer function $G(s)$ is obtained, as presented in Eq. (9). This function relates the output voltage $v_{C2}(s)$ with the switching signal $\alpha(s)$.

Table 1. System parameters

Parameter	Symbol	Value
Load power		2 kW
Input DC voltage		90 V
Switching frequency		50 kHz
Duty ratio		0.355
Output DC voltage		48 V
Output current	-	41.67 A
		10 A
		0.95 V, 0.96 V
		80 µH
		50 mΩ
		330 µF
		680 µF
Load (Resistor)		1.15 Ω

$$G(s) = \frac{-1.058x10^{21}s^3 + 4.711x10^{25}s^2 + 2.102x10^{28}s + 1.218x10^{33}}{1.11x10^{16}s^4 + 3.27x10^{19}s^3 5.618x10^{23}s^2 + 8.405x10^{26}s + 6.042x10^{30}}$$ (9)

The controller that improves the dynamic response of the converter is designed based on the root locus technique using MATLAB® RLTOOL. The controller design specifications include a settling time at output voltage v_{C2} of 25ms with 0% override.

To satisfy the control objective, a PI controller with constants $K_p = 0.00035$ and $K_I = 0.686$ is used. By performing the feedback described in Figure 3, the closed-loop response of the SEPIC converter is obtained in the state space representation loaded in the block called SEPIC. The control signals and the input voltage signal V_s enter

this block. Variations in the voltage signal V_s are enacted through the step signal with amplitudes of 85 and 90 V. The proposed control scheme allows the voltage to be regulated to 48 V.
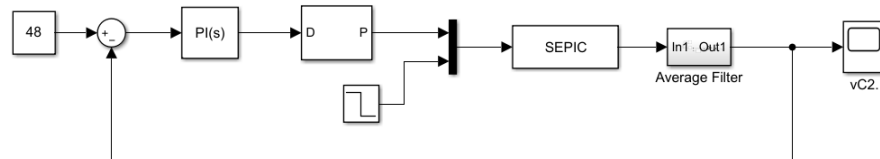

Figure 3. Scheme control used in the SEPIC converter.

Figure 4 illustrates the SEPIC converter circuit. Circuit simulation was performed in MATLAB SIMULINK using the TOOLBOX SIMSCAPE. To change the input circuit voltage, a source controlled by a step signal was used.
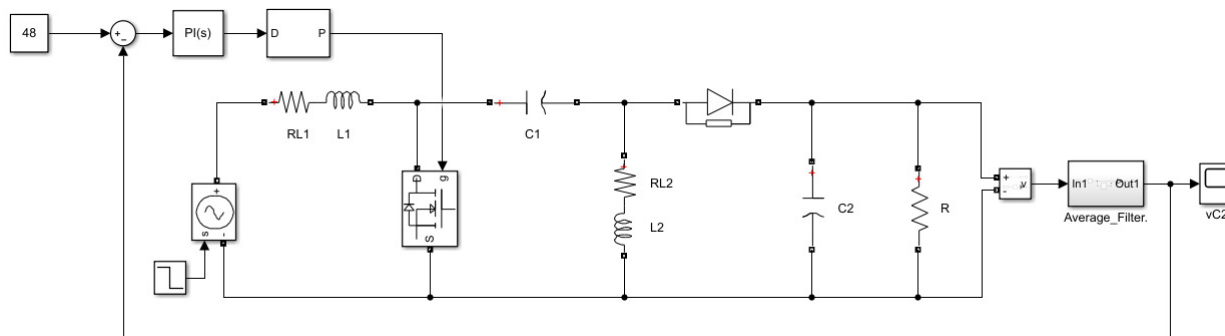

Figure 4. Controlled SEPIC converter circuit.

Due to the switching action of the control signal, a filter is incorporated at the output of the SEPIC converter that obtains the average value of the voltage signal. The simulation results are shown in the next section.

Results

This section presents the simulation results of the SEPIC converter with a 2-kW load using the MATLAB®/ SIMULINK® simulation tool, using the values of the converter parameters shown in Table 1. Figure 5 displays the open-loop output voltage of the mathematical model and the SEPIC converter circuit. At time 80 ms the input DC voltage changes to 85 V. According to Eq. (5), the output voltage of the converter in steady state v_{C2e} is directly proportional to the input voltage; therefore, the output voltage is reduced.
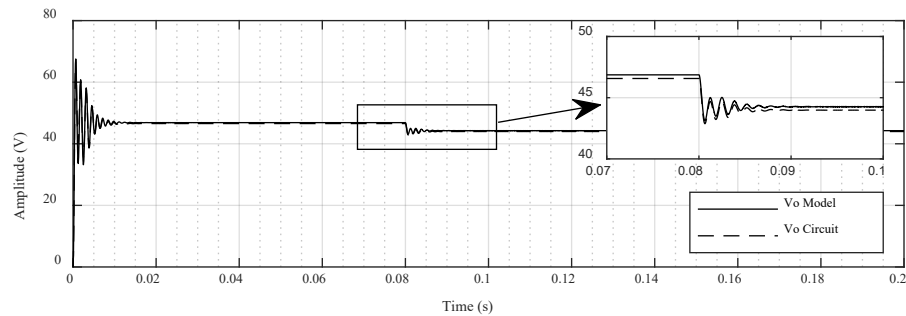
Figure 5. Open loop response of the proposed model and the SEPIC converter circuit.

The output voltage of the SEPIC converter controlled for the model and the converter circuit using discrete elements is shown in Figure 6. The initial configuration of the converter is established with the parameters in Table 1. At the time instant 80 ms, the input voltage changes to 85 V. The simulation results demonstrate that the settling time for both the model and the circuit is less than 25 ms, indicating that the proposed controller satisfies the design specifications around the operating point.
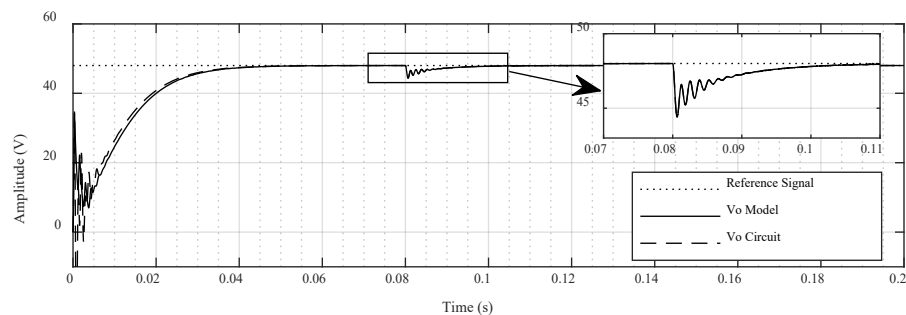

Figure 6. Controlled SEPIC converter response.

Figure 7 shows the controller's output signal. The magnitudes of the control signals for the proposed model and the simulated circuit with discrete elements are less than 0.5 V. Therefore, the controller could be implemented in either an analog or digital manner.
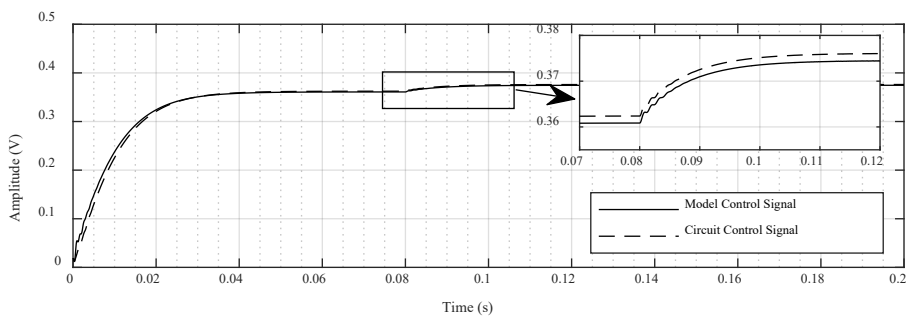

Figure 7. Control signal against disturbances in SEPIC controller.

Figure 8 illustrates the controlled converter's response to load changes. During the 0 to 100 ms interval, the charge corresponds to 1.15 Ω; however, from time point 80

ms onwards, it increases by 5%. The simulation results show that the proposed PI controller regulates the output voltage in the face of changes close to the established operating point, specifically in the DC input voltage and the load connected to the converter.
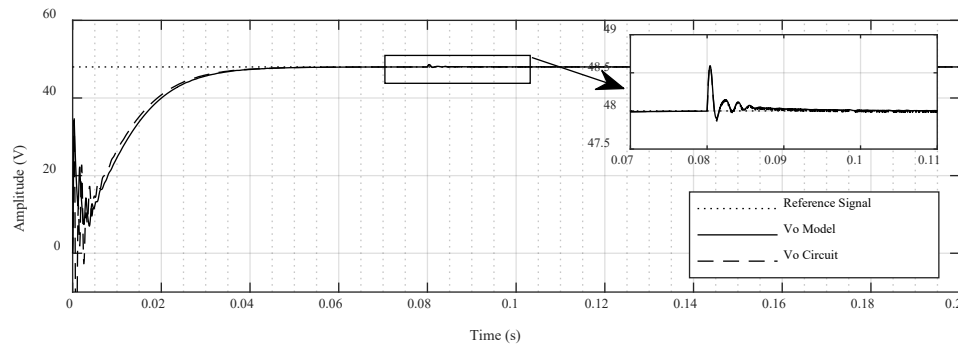

Figure 8. SEPIC converter output voltage by adjusting load magnitude.

Conclusions

The mathematical model proposed in this article incorporates the internal resistances of the inductors, providing a closer approximation to the physical implementation of the converter. This enhancement enables more precise controller design to meet the desired specifications, as the operational point of the SEPIC converter involves more variables than the associated dynamics.

The model presented can be applied in the analysis of renewable energy systems, energy storage, and systems interconnected to the grid. Such applications require an analysis of the efficiency and performance of control systems in mitigating disturbances caused by the load or the DC power supply.

The simulation results indicate that the proposed controller can be implemented in both analog or digital systems. This is evident as the controller effort signal remains below 0.4 V for the configurations established around the operating point variations.

References

1. Mumtaz F, Zaihar Yahaya N, Tanzim Meraj S, Singh B, Kannan R, Ibrahim O. Review on non-isolated DC-DC converters and their control techniques for renewable energy applications. Ain Shams Engineering Journal. 2021;12(4):3747-63. https://doi.org/10.1016/j.asej.2021.03.022

2. Sivakumar S, Sathik MJ, Manoj PS, Sundararajan G. An assessment on performance of DC-DC converters for renewable energy applications. Renewable and Sustainable Energy Reviews. 2016;58:1475-85. https://doi.org/10.1016/j.rser.2015.12.057

3. Mouslim S, Oubella M, Kourchi M, Ajaamoum M. Simulation and analyses of SEPIC converter using linear PID and fuzzy logic controller. Materials Today: Proceedings. 2020;27:3199-208.https://doi.org/10.1016/j.matpr.2020.04.506

4. Ayachit A, Reatti A, Kazimierczuk MK. Small-signal modeling of PWM dual-SEPIC dc-dc converter by circuit averaging technique. In: IECON 2016 - 42nd Annual Conference of the IEEE Industrial Electronics Society. 2016. p. 3606-11. https://doi.org/10.1109/IECON.2016.7793030

5. Polsky T, Horen Y, Bronshtein S, Baimel D. Transient and Steady-State Analysis of a SEPIC Converter by an Average State-Space Modelling. In: 2018 IEEE 18th International Power Electronics and Motion Control Conference (PEMC). 2018. p. 211-5. https://doi.org/10.1109/EPEPEMC.2018.8522000

6. Kanimozhi G, Meenakshi J, Sreedevi VT. Small Signal Modeling of a DC-DC Type Double Boost Converter Integrated with SEPIC Converter Using State Space Averaging Approach. Energy Procedia. 2017;117:835-46. https://doi.org/10.1016/j.egypro.2017.05.201

7. Poluthai S, Jirasuwankul N. Simulation of a Miniature SEPIC Converter with PI Controller for Thermoelectric Generator Module. In: 2018 International Electrical Engineering Congress (iEECON). 2018. p. 1-4. https://doi.org/10.1109/IEECON.2018.8712248

8. Hussain J, Mishra MK. Design of current mode controlled SEPIC DC-DC converter for MPPT control of wind energy conversion systems. In: 2015 International Conference on Computation of Power, Energy, Information and Communication (ICCPEIC). 2015. p. 177-82. https://doi.org/10.1109/ICCPEIC.2015.7259460

9. Geethalakshmi B. Design of a closed loop control scheme for a DC-DC SEPIC converter using loop shaping method. In: 2015 International Conference on Circuits, Power and Computing Technologies [ICCPCT-2015]. 2015. p. 1-5. https://doi.org/10.1109/ICCPCT.2015.7159361

10. Sivamani D, Ramkumar R, Nazar Ali A, Shyam D. Design and implementation of highly efficient UPS charging system with single stage power factor correction using SEPIC converter. Materials Today: Proceedings. 2021;45:1809-19. https://doi.org/10.1016/j.matpr.2020.08.744

11. Sel A, Güneş U, Elbir Ö, Kasnakoğlu C. Comparative analysis of performance of the SEPIC converter using LQR and PID controllers. In: 2017 21st International Conference on System Theory, Control and Computing (ICSTCC). 2017. p. 839-44. https://doi.org/10.1109/ICSTCC.2017.8107141

12. Chandan B, Dwivedi P, Bose S. Closed Loop Control of SEPIC DC-DC Converter Using Loop Shaping Control Technique. In: 2019 IEEE 10th Control and System Graduate Research Colloquium (ICSGRC). 2019. p. 20-5. https://doi.org/10.1109/ICSGRC.2019.8837093

13. Gayen PK, Roy Chowdhury P, Dhara PK. An improved dynamic performance of bidirectional SEPIC-Zeta converter based battery energy storage system using adaptive sliding mode control technique. Electric Power Systems Research. 2018;160:348-61. https://doi.org/10.1016/j.epsr.2018.03.016

14. Elsayad N, Moradisizkoohi H, Mohammed O. A New SEPIC-Based Step-Up DC-DC Converter with Wide Conversion Ratio for Fuel Cell Vehicles: Analysis and Design. IEEE Transactions on Industrial Electronics. 2021;68(8):6390-400. https://doi.org/10.1109/TIE.2020.3007110

15. Arany RR, Bratcu AI. Robust control of a single-ended primary-inductor converter (SEPIC). In: 2017 5th International Symposium on Electrical and Electronics Engineering (ISEEE). 2017. p. 1-6. https://doi.org/10.1109/ISEEE.2017.8170665

16. Ullah M, Ulasyar A, Zad HS, Khattak A. Design of Linear Quadratic Regulator Controller for Sepic Converter. In: 2019 15th International Conference on Emerging Technologies (ICET). 2019. p. 1-6. https://doi.org/10.1109/ICET48972.2019.8994463

17. Bacha S, Munteanu I, Bratcu AI. "Power Electronic Converters Modeling and Control", Advanced Textbooks in Control and Signal Processing. London: Springer; 2014. https://doi.org/10.1007/978-1-4471-5478-5

18. Kircioğlu O, Ünlü M, Çamur S. Modeling and analysis of DC-DC SEPIC converter with coupled inductors. In: 2016 International Symposium on Industrial Electronics (INDEL). 2016. p. 1-5. https://doi.org/10.1109/INDEL.2016.7797807

19. Verma M, Kumar SS. Hardware Design of SEPIC Converter and its Analysis. In: 2018 International Conference on Current Trends towards Converging Technologies (ICCTCT). 2018. p. 1-4. https://doi.org/10.1109/ICCTCT.2018.8551052

20. Nishat MM, Oninda MAM, Faisal F, Hoque MA. Modeling, Simulation and Performance Analysis of SEPIC Converter Using Hysteresis Current Control and PI Control Method. 2018 International Conference on Innovations in Science, Engineering and Technology, ICISET 2018. 2018;(October):7-12.

21. Goudarzian A, Khosravi A, Raeisi HA. A new approach in design of sliding-mode voltage-controller for a SEPIC. International Journal of Dynamics and Control. 2021;9(3):1197-209. https://doi.org/10.1007/s40435-020-00741-9

22. Sree BL, Umamaheswari MG. Modeling and control of solar power fed single ended primary inductor converter using cascade control scheme. In: 2017 Trends in Industrial Measurement and Automation (TIMA). 2017. p. 1-7. https://doi.org/10.1109/TIMA.2017.8064784